Revision-02

Tetrataenite in terrestrial rock

BIBHURANJAN NAYAK[1,*] AND FRANZ MICHAEL MEYER[2]

[1]Mineral Processing Division, CSIR National Metallurgical Laboratory, Jamshedpur-831007, India

[2]Institute of Mineralogy and Economic Geology, RWTH Aachen University, D-52056 Aachen, Germany

* E-mail: brn69@rediffmail.com, brn@nmlindia.org

ABSTRACT

Tetrataenite is an equiatomic and highly ordered, non-cubic Fe-Ni alloy mineral that forms in meteorites from the distortion of fcc taenite due to extremely slow cooling. The mineral has drawn much attention of the scientific community because of its superb magnetic properties, which may make the phase an alternative to the REE-based permanent magnets. Barring only a few passing mentions, the mineral has never been described from any terrestrial rock. Here we report the characteristics of terrestrial tetrataenite from an ophiolite-hosted Ni-bearing magnetite body from the Indo-Myanmar ranges, northeast India. Although the mineral assemblage surrounding it is very similar to that found in the meteorites, the postulated cooling regimes cannot be similar. The mineral is formed as a consequence of hydrothermal alteration of ferromagnesian minerals of the olivine and pyroxene groups. Iron and nickel were released from the silicates and precipitated in the form of Fe-Ni alloy at low temperature in extremely reducing conditions with a lack of sulfur. Our findings suggesting a low-temperature hydrothermal origin of tetrataenite warrants a re-examination of the Fe-Ni phase diagram at low temperatures, and puts a question mark on the age-old concept of tetrataenite formation as due solely to extremely slow cooling of fcc taenite in meteorites. It also opens up a new vista for adoption of a hydrothermal route to synthesize this rare material.

Keywords: Tetrataenite, Fe-Ni alloy, hydrothermal, terrestrial, Ni-bearing magnetite

INTRODUCTION

Metallic Fe-Ni alloy is ubiquitous in meteorites although its modal abundance is less than 1 vol. % (Heiken et al. 1991). The Fe-Ni alloy minerals commonly found in meteorites are kamacite and taenite. Kamacite is characterized by a relatively low Ni-content (< 7 wt. %) and a body-centered cubic (bcc) structure (the α-phase). Taenite contains up to about 55 wt. % Ni and has a face-centered cubic (fcc) structure (the γ-phase). In terrestrial rocks, metallic Fe-Ni is rare and found only in serpentinized peridotites (Krishnarao 1964; Frost 1985) and volcanic rocks that have assimilated carbonaceous material; both are environments in which there is substantial reducing potential due to the presence of H_2 and C (Goodrich and Bird 1985). The compositions of these alloy minerals in terrestrial rocks are predominantly restricted to the awaruite group (Ni_2Fe to Ni_3Fe) with variable Fe/Ni ratios where Ni concentrations sometimes reach up to 75 wt.% (Staples 1962). Tetrataenite, an equiatomic and highly ordered Fe-Ni alloy mineral that generally forms from the distortion of fcc taenite, has been established as a distinct mineral phase in some meteorites (Albertsen et al. 1978a, b; Clarke Jr. and Scott 1980). With ~51 wt.% Ni, it presents a tetragonal structure (superstructure $L1_0$ like CuAu), space group P4/mmm; a = 2.533 Å and c = 3.582 Å (Albertsen et al. 1978a). Tagai et al. (1988, 1995), however, argued that tetrataenite is only metrically tetragonal and its structure has monoclinic symmetry. The mineral is found mainly in extremely slowly cooled meteorites (cooling rate of a few degrees per million years for the temperature interval of 700–350 ºC; Wood 1964; Goldstein and Short 1967), and is formed

when meteorites cool slowly below 320 ºC, which is the order-disorder transition temperature (Zhang et al. 1990). The cooling below 320 °C could be even slower and is important for the ordering of Ni and Fe in the atomic structure. Since below this temperature the auto-diffusion in the Fe–Ni system is insignificant on laboratory time scales, tetrataenite cannot be produced artificially by simple annealing of compositionally equivalent taenite phase with a disordered structure. Therefore, significant amounts of tetrataenite are found only in meteoritic samples that have suffered a slow and very long cooling process (Scorzelli 1997). Although this ultra-rare Fe-Ni phase can be produced in a small scale synthetically by neutron- or electron-irradiation of Fe-Ni alloys at temperatures below 593 K (Pauleve et al. 1962; Gros and Pauleve 1970; Chamberod et al. 1979), or by hydrogen-reduction of nanometric $NiFe_2O_4$ (Lima Jr. et al. 2003), its large-scale production has not been achieved as of now. To the best of our knowledge, to date, tetrataenite has never been described from terrestrial rocks barring only a few mentions (Tominaga and Klein 2011; Rajabzadeh and Moosarinasab 2013). In this note we report the identification of tetrataenite in an ophiolite-hosted, Ni-bearing magnetite body from the Indo-Myanmar ranges of northeast India and discuss its characteristics, mode of occurrence, chemistry, and genesis, as well as the possible technological consequences of its occurrence in such an environment.

METHODS OF INVESTIGATION

Five samples from the magnetite body were investigated using a Leica optical petrological microscope. Quantitative microchemical compositions of the mineral phases were determined by an electron probe micro-analyzer (EPMA; JEOL Superprobe JXA-8900R having five numbers of WDX and one EDX spectrometers) using WDX and suitable

standards. The relative percent error was less than 1% in all cases. Whereas magnetite, chromite and other spinels were measured against a magnetite standard, the sulfides were measured against a chalcopyrite standard and the metallic alloys were measured against metal standards with a focused beam of 1.6 μm diameter and accelerated voltage of 25 kV. Measurements were taken for 10 sec with background time of 5 sec and probe current was kept at 27 nA. For chamosite, a chlorite standard was used and the beam diameter was kept at 10 μm in order to accommodate more area, because chlorite with its hydrous structure is likely to suffer more from beam damages with a focused beam. The electron backscatter diffraction (EBSD) pattern of the tetrataenite crystal was obtained using a JEOL JSM 7000F SEM with a combined EDX/EBSD system provided by EDAX-TSL, consisting of a 'Sapphire' Si(Li)-EDX-detector and a 'Hikari' EBSD camera. The mineral was investigated keeping the sample stage tilted at an angle of 70°, and data were collected using OIM (Orientation imaging microscopy) software – Data Collection V 6.2. The data file for magnetite came from the built-in database, and the tetrataenite file came from the American Mineralogist Crystal Structure (AMCS) Database. The Kikuchi patterns were recorded at beam energy of 20 keV and around 30 nA beam current. For the EBSD camera we used a 2x2 binning of the pixels and a combined background correction (background subtraction, dynamic background subtraction and normalize intensity histogram). Quantitative volume fractions of various mineral phases were determined using an FEI QEMSCAN 650F with two EDAX attachments (Bruker 133eV). Measurements were taken using a 5-μm grid with 2000 counts/sec at an accelerated voltage of 25 kV. Since data generated from XRD, XRF and ICPMS do not form a part of this article, the methodologies for such investigations are not included here.

CHARACTERISTICS OF TETRATAENITE

The occurrence of a tetrataenite crystal was first confirmed from its composition measured by EPMA, while investigating a Ni- and Cr-bearing magnetite sample from the Pokphur magnetite body that occurs in the north-eastern most part of the Nagaland-Manipur ophiolite belt, a part of the Indo-Myanmar ranges in north-eastern India. It shows a cream color and high reflectivity (Fig. 1), and is distinctly anisotropic under cross nicols. These optical properties are characteristic of tetrataenite and allow it to be distinguished from cubic taenite that shows a dark grey color with very low reflectivity and is isotropic under cross nicols. The chemical composition of the crystal was determined by EPMA using WDX and metal standards. The analyses revealed an average of 50.5 wt.% Ni (Table 1), which is close to the theoretical Ni concentration of tetrataenite (51.24 wt.% Ni). Extraterrestrial tetrataenite generally contains some Co (0.02 to 2.0 wt.%) and Cu (0.11 to 0.36 wt.%) as impurities (Clarke and Scott 1980). However, in this case Co and Cu concentrations are significant, about 8 and 3 wt.%, respectively (Table 1). We take this as evidence of a different generation of this mineral in the terrestrial setting. The SEM image of the crystal shows a euhedral shape with the longer sides parallel to the *c*-axis direction (Fig. 2) and the other two sides diverging, forming a trapezoidal cross section. Barring only one instance in the Jelica meteorite, tetrataenite mostly occurs in anhedral shapes because of its replacement origin from fcc taenite and several restrictive conditions prevailing during its formation (Rubin 1994). However, in the present terrestrial case tetrataenite occurs as an independent single crystal associated with altered silicates in a cavity within a mass of magnetite. Back-scattered electron image and X-ray elemental mapping show that the crystal has a uniform composition

throughout (see supplementary Figs. 1 and 2). Since Ni accounts for about 51 wt.% of the grain (close to the stoichiometric ratio), it is apparent that Co and Cu occupy some of the Fe-sites in the crystal structure. To identify its structure, the grain was investigated by SEM with electron backscatter diffraction (EBSD) facility. The EBSD Kikuchi pattern thus obtained (Fig. 3) was indexed; it fits well with the mineral (tetrataenite) having a tetragonal symmetry. The Kikuchi patterns of fcc taenite cannot generally be distinguished from that of tetrataenite using EBSD, because the ordering of Fe and Ni causes only a very small distortion of the parent taenite structure and the *c*/*a* ratios in both cases are very close (~1.0036) (Albertsen 1981; Goldstein and Michael 2006). However, although the Kikuchi pattern obtained in the present case can also perhaps be indexed as fcc taenite, the characteristic optical properties and the chemical composition of this phase precludes it to be fcc taenite, which contains only about 25-40 wt.% Ni.

GEOLOGY AND PETROGRAPHY OF THE MAGNETITE BODY

In the Naga Hills ophiolites, the magnetite body occurs as discontinuous thin sheets extending about a kilometer in strike length over a cumulate sequence of meta-ultramafics (Chattopadhyay et al. 1983). The thickness of the body varies from 5 to 12 m with an average outcrop width of about 300 m. The underlying rocks are composed of dunite, harzburgite, lherzolite, olivine-pyroxenite, pyroxenite, and amphibolite. The magnetite body is hard, massive and jointed. It shows a broad synformal warp with slickensides and groove lineations suggestive of small-scale gliding. Optical microscopic studies reveal that the samples collected from the magnetite body consists of magnetite and lesser amounts of chromite dispersed in a matrix of Fe-chlorite (chamosite). These three minerals constitute about 95

vol.% of the samples (62.2 vol.% chamosite, 30.6 vol.% magnetite, and 1.9 vol.% chromite averaging five samples; supplementary Figs. 3 to 7). In general, this Fe-chlorite contains significant concentrations of Cr (supplementary Table 1), which has also been reported by earlier workers (Mohapatra et al. 1995). Although the Mg and Cr concentrations in Fe-chlorite are generally low (<2 wt.% MgO; <0.5 wt.% NiO) and irregularly distributed, the particular sample in which terataenite is found contains relatively high Mg and Ni concentrations (~5 wt.% MgO; ~2 wt.% NiO), and is characterized by higher magnetite abundance. Chromite occurs as discrete grains scattered throughout the magnetite- and chamosite-rich portions. In the majority of cases, chromite has been replaced by magnetite, both at grain boundaries and along fracture planes, leaving corroded remnants of chromite grains (Fig. 4). This textural relation strongly indicates that magnetite formed later than chromite. The alteration and replacement of chromite is thought to be the source of Al and Cr in the Fe-chlorite because the unaltered chromite grains in these samples are alumina-rich (18 to 27 wt.% Al_2O_3). Locally, the magnetite grains are also partly martitized due to late-stage supergene oxidation. Other less abundant minerals recorded are mangan-ilmenite, hercynite, maghemite, goethite and rutile. Sulfides are rare indicating a low-S environment; only traces of chalcocite (Cu_2S; ~80 wt.% Cu, ~20 wt.% S) and non-stoichiometric compositions of Fe-Ni-S and Fe-Ni-Co-S were recorded. However, occurrences of fine-grained metallic alloys (< 25 μm), mostly represented by Cu-Fe (~93 wt.% Cu and ~7 wt.% Fe), were observed more frequently, although their modal abundance is very low (< 0.5 vol.%). The metal alloys and sulfides are always found to be restricted to the spinels, either magnetite or Cr-Al spinel (Fig. 5; supplementary Figs. 8 and 9). Many extremely fine-grained metallic and/or sulfide inclusions (< 5 μm), whose compositions could not be determined precisely by EPMA, also occur in

these spinels. The spinels in which metallic alloys/sulfides were recorded are always found to have corroded margins and show some degree of alteration. Only one occurrence of tetrataenite was observed in the form of a euhedral single crystal within a cavity surrounded by altered silicates in a mass of magnetite (Fig. 2).

ORIGIN OF TETRATAENITE

The cumulate complex with which the magnetite body is associated consists primarily of ultramafic rocks such as dunite, harzburgite, lherzolite, olivine-pyroxenite, pyroxenite, and amphibolite containing various proportions of olivine, orthopyroxene, clinopyroxene, amphibole, biotite, epidote and plagioclase. Due to metamorphism (greenschist to amphibolite facies) these rocks are altered to different extents at different places. In such dunitic rocks, fractured and corroded olivine grains are often surrounded and traversed by serpentine (lizardite and antigorite) veinlets (Chattopadhyay et al. 1983). Rounded grains of magnetite are distributed along olivine grain boundaries and within serpentine veinlets, suggesting that the excess iron released during serpentinization of olivine formed iron oxide. Mobility of Fe and formation of magnetite during hydrothermal alteration of olivine is not uncommon (Gahlan et al. 2006; Evans et al. 2013; McCollom and Seewald 2013). From the textures of the magnetite samples studied here, it is apparent that the magnetite body has formed by a similar process due to hydrothermal alteration of olivine and pyroxene. Since the matrix of the magnetite ore is composed of Fe-chlorite only, with very low Mg content, it is inferred that the original olivine could have been of fayalitic composition. Whether or not the P, T, t conditions of alteration are comparable between ophiolites and meteorites, the similarity in their matrix phase assemblages (eg. anhydrous and hydrous ferromagnesian silicates) is rather

striking. For example, Abreu (2012), and Abreu et al. (2014) have shown that shock metamorphism followed by hydrothermal alteration by fluids released during impact can produce similar mineral assemblages in CR2 chondrites. The opaque minerals (including taenite and tetrataenite) they found in GRA 06100 (a CR chondrite) are associated with anhydrous silicates such as fayalite and ferrosilite and hydrous silicates such as serpentine and non-stoichiometric ferromagnesiosilica. The duration of thermal metamorphism of the chondrites could be for a short duration (Briani et al. 2013). Olivine is also a common phase in many meteorites, and serpentine is the dominant hydroxyl-bearing mineral in CM carbonaceous chondrites (Calas 2013). That the process of serpentinization (and chloritization) is accompanied by conditions of extremely low fO_2 has been noted by many authors (Frost 1985; Sleep et al. 2004; Evans et al. 2013; McCollom and Seewald 2013). This conclusion is based not only upon the widespread occurrence of native metals in serpentines, but also on the occurrence of H_2 gas in springs draining areas of active serpentinization (Barnes et al. 1972; McCollom and Seewald 2013; Schrenk et al. 2013). Most authors attribute the occurrence of a reducing environment to the fact that a reaction such as

$$6\ Fe_2SiO_4 + 7\ H_2O = 3\ Fe_3Si_2O_5(OH)_4 + Fe_3O_4 + H_2 \quad (1)$$

olivine serpentine magnetite

occurs during serpentinization and that the hydrogen released by this reaction acts as the reducing agent. Under proper conditions the strong gradient in fO_2 can lead to mobilization of metals or sulfides. Josephinite nodules, for example, are postulated to have formed during high-temperature, reversible serpentinization. In such a situation, the location of the serpentinization front and its associated environment of extreme reduction will be thermally fixed, forming a site for deposition of native metals (Frost 1985). The reduction associated

with serpentinization is caused by the fact that serpentinization of olivine involves the production of magnetite and this, by necessity, induces reduction of the associated fluid phase. In the present case, since the Fe-Cu and Fe-Ni alloy minerals are found as inclusions either within magnetite or altered Fe-Mg-Al-Cr spinels (other than chromite *sensu stricto*), it is apparent that these have not directly crystallized from a magmatic source. Because of their association with altered and secondary phases, they appear to have formed during hydrothermal alteration that converted olivine and pyroxene to Fe-chlorite and formed secondary Fe-Mg-Al-Cr spinels and magnetite. The excess Cu, Ni, Co and Fe that could not be accommodated within the structure of magnetite or spinel got exsolved and formed inclusions in the form of alloys. As far as the tetrataenite crystal is concerned, it is neither associated with any extraterrestrial minerals like kamacite or taenite nor shows any pseudomorphous character, thereby ruling out any possibility of cosmic origin. Moreover, the chemical composition (high Cu and Co content) of this tetrataenite is quite different from extraterrestrial examples, which precludes it being a contaminant from any extraterrestrial material. Its occurrence within a cavity surrounded by altered silicates in a mass of magnetite suggests that the mineral precipitated from Ni- and Fe-bearing hydrothermal solution at low temperatures under extremely reducing conditions. Nickel and Fe could be released from the Ni-bearing silicates (eg. olivine and pyroxene) due to hydrothermal alteration and re-precipitated to form tetrataenite. Since the mineral has precipitated in a cavity, it could grow to an almost perfect crystal without hindrance. Tetrataenite, in this case, could be the youngest in the paragenetic sequence. P-T conditions derived from PERPLEX modeling showed the stability of the assemblage ferrochromite, ferrobrucite, ferrochlorite at < 280 °C and 1 kb pressure (supplementary Fig. 10). It has been shown experimentally (Andreani et al. 2013)

that olivine dissolution is enhanced by the presence of dissolved Al in the fluid, and this could lead to the precipitation of Al-rich hydrated silicates such as chlorite. The stability of fayalite-rich olivine was found to extend to temperatures as low as 180 °C in the presence of water (Klein et al. 2013). Using these circumstantial evidences it is concluded that the reaction forming tetrataenite may have occurred at temperatures even below 280 °C. A possible mineral reaction could be

$$12\ Fe_2SiO_4 + 28\ H_2O + 8\ Al\ (\text{from Cr-spinel}) + Ni\ (\text{from olivine}) =$$

$$4\ Fe_5Al_2Si_3O_{10}(OH)_8 + Fe_3O_4 + FeNi + 12\ H_2 \qquad (2)$$

An astounding amount of literature is available on the Fe-Ni phase diagrams. However, the stability fields of Fe-Ni alloys are not well established at low temperatures, especially below 400 °C, and there has been discussion as to whether tetrataenite (the γ''-phase) is stable or metastable (Reuter et al. 1989; Yang et al. 1996; Howald 2003; Mishin et al. 2005). Although recent thermodynamic calculations indicate that the γ''-phase is metastable, it would only take a 300 J/mol (~0.003 eV/atom) decrease in the free energy to make this phase stable at room temperature (Howald 2003). Although an assessment of hydrothermal fluid equilibria with Fe-Ni alloys has not been possible due to the lack of solubility data for these phases (Klein and Bach 2006), using standard formation thermochemical data, Howald (2003), however, has shown that tetrataenite has a region of stability in the equilibrium phase diagram. Hence, the occurrence of tetrataenite is not impossible in terrestrial conditions, and a deliberate search for terrestrial tetrataenite in similar environments can (perhaps) provide more examples.

Implications

Our interpretation on the hydrothermal precipitation of tetrataenite in a crustal rock warrants a re-examination of the Fe-Ni phase diagram at low temperatures, and puts a question mark on the age-old concept of tetrataenite formation as due solely to extremely slow cooling of fcc taenite in meteorites. Some of the Fe-Ni phases observed by Abreu et al. (2014) in the CR2 chondrites could also be due to hydrothermal alteration. Tetrataenite, the equiatomic FeNi phase with chemically-ordered $L1_0$ tetragonal structure, is a highly promising material for future-generation, rare-earth-free permanent magnets. Permanent magnets that convert mechanical to electrical energy and *vice versa* are used in satellite positioning systems, motors for hybrid and electric vehicles, wind turbines, hard disk drives, and many defense applications (Lewis and Jiménez-Villacorta 2013). Present day permanent magnets require rare-earth elements, but due to various geopolitical factors their availability is in jeopardy. $L1_0$-structured FeNi would be an advantageous permanent magnetic material because both Fe and Ni are inexpensive and readily available. Although many research groups across the world are actively engaged in finding ways to produce this alloy, no breakthrough has been achieved and mass production has not been a success as yet since this phase was first synthesized by neutron irradiation in minute quantity in the 1960s (Néel et al. 1964; Yang et al. 1996; Lima Jr. et al. 2003). Taking lessons from this terrestrial tetrataenite, we suggest that a low-temperature hydrothermal synthesis route might be feasible to produce this rare Ni-Fe alloy which would reduce the dependency on REE-based permanent magnets.

Supplementary Information is provided in a separate file

ACKNOWLEDGEMENTS

Preliminary work carried out at the CSIR National Metallurgical Laboratory, Jamshedpur, India was followed with a detailed investigation at the Institute of Mineralogy and Economic Geology, RWTH Aachen University, Germany where facilities such as EPMA, XRF, QEMSCAN, ICP-MS and XRD were utilized. Roman Klinghardt, Dr. Sven Sindern, Nicolas Stoltz, Lars Gronen, and Dr. Andre Hellmann assisted in operating the analytical equipment. Thomas Derichs prepared the polished sections. EBSD data were generated at the GFE, RWTH Aachen and we thank Dr. Alexander Schwedt for extending the support. Dr. S. Srikanth, Director, CSIR-NML is thanked for encouraging to undertake a research project on Nagaland magnetite deposit. The visit of B. Nayak to RWTH was financially supported by the Alexander von Humboldt Foundation, Bonn, Germany. Constructive comments of Dr. Alan E. Rubin, Dr. Kula C. Misra and Dr. Ian Swainson markedly improved the quality of this manuscript.

REFERENCES CITED

Abreu, N.M. (2012) Low and high temperature aqueous alteration of the matrices of CR chondrites: Nano-SEM, EPMA, and TEM study. Lunar and Planetary Science, 43, 2739 (abstr.)

Abreu, N.M., Bland, P.A., and Rietmeijer, F.J.M. (2014) Effects of shock metamorphism on the matrix of CR chondrites: GRA 06100. Lunar and Planetary Science, 45, 2753.

Albertsen, J.F. (1981) Tetragonal lattice of tetrataenite (ordered Fe-Ni, 50-50) from 4 meteorites. Physica Scripta, 23, 301-306.

Albertsen, J.F., Aydin, M., and Knudsen, J.M. (1978a) Mössbauer effect studies of taenite lamellae of an iron meteorite Cape York (IIIA). Physica Scripta, 17, 467-472.

Albertsen, J.F., Jensen, G.B., and Knudsen, J.M. (1978b) Structure of taenite in two iron meteorites. Nature, 273, 453-454.

Andreani, M., Daniel, I., and Pollet-Villard, M. (2013) Aluminum speeds up the hydrothermal alteration of olivine. American Mineralogist, 98, 1738–1744.

Barnes, I., Rapp, J.B., O'Neil, J.R., Sheppard, R.A., and Gude, A.J. (1972) Metamorphic assemblages and the direction of flow of metamorphic fluids in four instances of serpentinization. Contributions to Mineralogy and Petrology, 35, 263-76.

Briani, G., Quirico, E., Gounelle, M., Paulhiac-Pison, M., Montagnac, G., Beck, P., Orthous-Daunay, F.-R., Bonal, L., Jacquet, E., Kearsley, A., and Russell, S.S. (2013) Short duration thermal metamorphism in CR chondrites. Geochimica et Cosmochimica Acta, 122, 267-279.

Calas, G. (2013) Editorial. Elements, 9, 83.

Chamberod, A., Laugier, J., and Penisson, J.M. (1979) Electron-irradiation effects on iron-nickel invar alloys. Journal of Magnetism and Magnetic Materials, 10, 139-144.

Chattopadhyay, B., Venkataramana, P., Roy, D.K., Bhattacharyya, S., and Ghosh, S. (1983) Geology of Naga Hills ophiolites. Records of the Geological Survey of India, 112, 59-115.

Clarke Jr., R.S., and Scott, E.R.D. (1980) Tetrataenite ordered FeNi, a new mineral in meteorites. American Mineralogist, 65, 624-630.

Evans, B.W., Hattori, K., and Baronnet, A. (2013) Serpentinite: what, why, where? Elements, 9, 99-106.

Frost, B.R. (1985) On the stability of sulfides, oxides, and native metals in serpentinite. Journal of Petrology, 26, 31-63.

Gahlan, H.A., Arai, S., Ahmed, A.H., Ishida, Y., Abdel-Aziz, Y.M., and Rahimi, A. (2006) Origin of magnetite veins in serpentine from the Late Proterozoic Bou-Azzar ophiolite, Anti-Atlas, Morocco: An implication for mobility of iron during serpentinization. Journal of African Earth Sciences, 46, 318-330.

Goldstein, J.I., and Michael, J.R. (2006) The formation of plessite in meteoritic metal. Meteoritics and Planetary Science, 41, 553–570.

Goldstein, J.I., and Short, J.M. (1967) The iron meteorites, their thermal history and parent bodies. Geochimica et Cosmochimica Acta, 31, 1733-1770.

Goodrich, C.A., and Bird, J.M. (1985) Formation of iron-carbon alloys in basaltic magma at Uivfaq, Disko Island: The role of carbon in mafic magmas. Journal of Geology, 93, 475-492.

Gros, Y., and Pauleve, J. (1970) Etude par effet Mössbauer de l'ordre dans un alliage Fe-Ni 50-50 irradié par des neutrons ou des électrons. Journal de Physique, 31, 459-470.

Heiken, G.H., Vaniman, D.T., and French, B.M. (eds). (1991) Lunar Sourcebook: A User's Guide to the Moon, Cambridge University Press, 736 pp.

Howald, R.A. (2003) The thermodynamics of tetrataenite and awaruite: A review of the Fe-Ni phase diagram. Metallurgical and Materials Transactions A, 34, 1759-1769.

Klein, F., and Bach, W. (2006) Opaque phase petrology and geochemical modeling as a guide to abiotic organic synthesis in the Mid-Atlantic Ridge 15N area: Results from ODP Leg 209. IODP-ICDP Kolloquium Griefswald, 27-29 March 2006, p.75.

345 Klein, F., Bach, W., and McCollom, T.M. (2013) Compositional controls on hydrogen
346 generation during serpentinization of ultramafic rocks. Lithos, 178, 55–69.
347 Krishnarao, J.S.R. (1964) Native nickel-iron alloy, its mode of occurrence, distribution and
348 origin. Economic Geology, 59, 443-448.
349 Lewis, L.H., and Jiménez-Villacorta, F. (2013) Perspectives on permanent magnetic materials
350 for energy conversion and power generation. Metallurgical and Materials Transactions
351 A, 44, 2-20.
352 Lima Jr., E., Drago, V., Fichtnerb, P.F.P., and Dominguesc, P.H.P. (2003) Tetrataenite and
353 other Fe–Ni equilibrium phases produced by reduction of nanocrystalline $NiFe_2O_4$.
354 Solid State Communications, 128, 345–350.
355 McCollom, T.M., and Seewald, J.F. (2013) Serpentinites, hydrogen, and life. Elements, 9,
356 129-134.
357 Mishin, Y., Mehl, M.J., and Papaconstantopoulos, D.A. (2005) Phase stability in the Fe-Ni
358 system: Investigation by first-principles calculations and atomistic simulations. Acta
359 Materialia, 53, 4029-4041.
360 Mohapatra, B.K., Rath, P.C., and Sahoo, R.K. (1995) Chromiferous chamosite from Pokphur
361 magnetite body, Nagaland, India. Current Science, 68, 1036-1039.
362 Néel, L., Paulevé, J., Pauthenet, R., Laugier, J., and Dautreppe, D. (1964) Magnetic properties
363 of an iron - nickel single crystal ordered by neutron bombardment. Journal of Applied
364 Physics, 35, 873-876.
365 Pauleve, J., Dautreppe, D., Laugier, J., and Néel, L. (1962) Etablissement d'une structure
366 ordonnée FeNi par irradiation aux neutrons. Comptes Rendus de l'Académie des
367 Sciences Paris, 254, 965-968.

368 Rajabzadeh, M.A., and Moosarinasab, Z. (2013) Mineralogy and distribution of platinum-
369 group minerals (PGM) and other solid inclusions in the Faryab ophiolitic chromitites,
370 Southern Iran. Mineralogy and Petrology, 107, 943-962.
371 Reuter, K.B., Williams, D.B., and Goldstein, J.I. (1989) Determination of the Fe-Ni phase
372 diagram below 400 °C. Metallurgical and Materials Transactions A, 20, 719-725.
373 Rubin, A. E. (1994) Euhedral tetrataenite in the Jelica meteorite. Mineralogical Magazine, 58,
374 215-221.
375 Schrenk, M.O., Brazelton, W.J., and Lang, S.Q. (2013) Serpentinization, carbon, and deep
376 life. Reviews in Mineralogy and Geochemistry, 75, 575-606.
377 Scorzelli, R.B. (1997) A study of phase stability in invar Fe–Ni alloys obtained by non-
378 conventional methods. Hyperfine Interactions, 110, 143–150.
379 Sleep, N.H., Meibom, A., Fridriksson, T.H., Coleman, R.G., and Bird, D.K. (2004) H_2-rich
380 fluids from serpentinization: Geochemical and biotic implications. Proceedings of the
381 National Academy of Sciences, 101, 12818-12823.
382 Staples, L.W. (1962) The discoveries of new minerals in Oregon. The Ore Bin, 24, 81-100.
383 Tagai, T., Takeda, H., Tokonami, M., Sasaki, S., and Danon, J. (1988) Determination of Fe
384 and Ni ordering in tetrataenite from Saint Severin meteorite using synchrotron
385 radiation. Notas de Física, Centro Brasileiro de Pesquisas Físicas-NF-044/88, 1-4.
386 Tagai, T., Takeda, H., and Fukuda, T. (1995) Superstructure of tetrataenite from the Saint
387 Severin meteorite. Zeitschrift für Kristallographie, 210, 14-18.
388 Tominaga, M., and Klein, F. (2011) Downhole magnetic and physical property logging of
389 serpentinized peridotite and carbonate-altered serpentinite. Workshop on Geological

Carbon Capture and Storage in Mafic and Ultramafic Rocks. 8-10 January 2011, Muscat, Oman (abstract No. 64).

Wood, J.A. (1964) The cooling rates and parent planets of several iron meteorites. Icarus, 3, 429-459.

Yang, C.W., Williams, D.B., and Goldstein, J.I. (1996) A revision of the Fe-Ni phase diagram at low temperatures (<400 ºC). Journal of Phase Equilibria, 17, 522-531.

Zhang, J., Williams, D.B., Goldstein, J.I., and Clarke Jr., R.S. (1990) Electron microscopy study of the iron meteorite Santa Catharina. Meteoritics, 25, 167–175.

TABLE 1. Chemical composition of tetrataenite by EPMA*

Element (wt.%)	**Point 1**	**Point 2**	**Point 3**	**Average**	**DL (ppm)**
Ag	0.02	0.00	0.01	0.01	117
Ni	50.46	50.42	50.59	50.49	152
Cu	2.95	3.76	2.86	3.19	119
Cd	0.02	0.01	0.01	0.01	105
Zn	0.00	0.00	0.00	0.00	208
Co	8.37	8.22	8.02	8.20	91
In	0.07	0.00	0.02	0.03	196
Au	0.00	0.07	0.02	0.03	191
Fe	36.71	36.43	37.93	37.02	82
Mn	0.12	0.12	0.11	0.12	84
Total	**98.72**	**99.03**	**99.57**	**99.10**	

* Error is < 1%; DL = Detection Limit

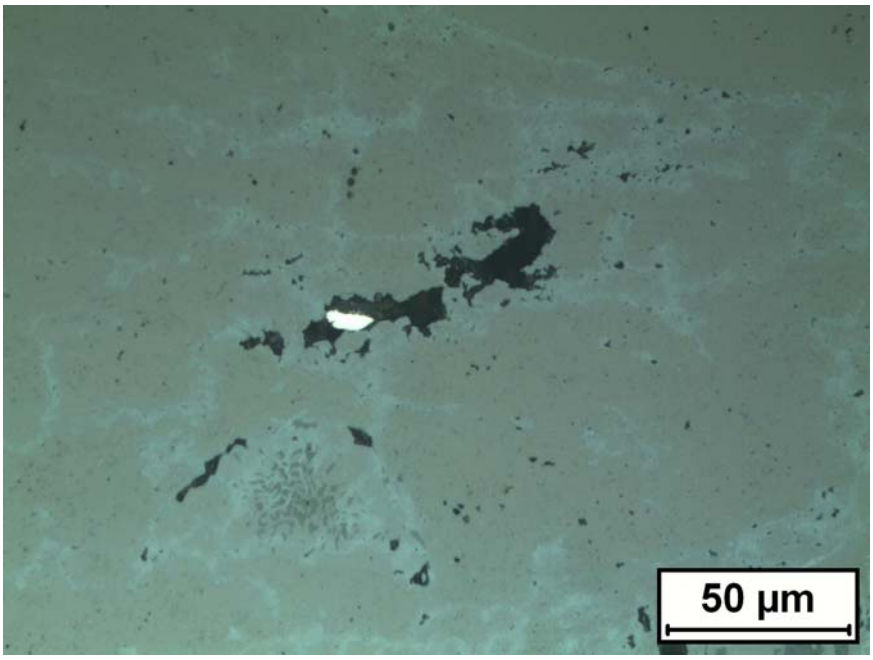

FIGURE 1. Occurrence of tetrataenite crystal (high reflectance) surrounded by Fe-chlorite (grey-black) within a cavity in a mass of magnetite. Reflected plane polarized light. Note the relicts of Cr-spinel within magnetite.

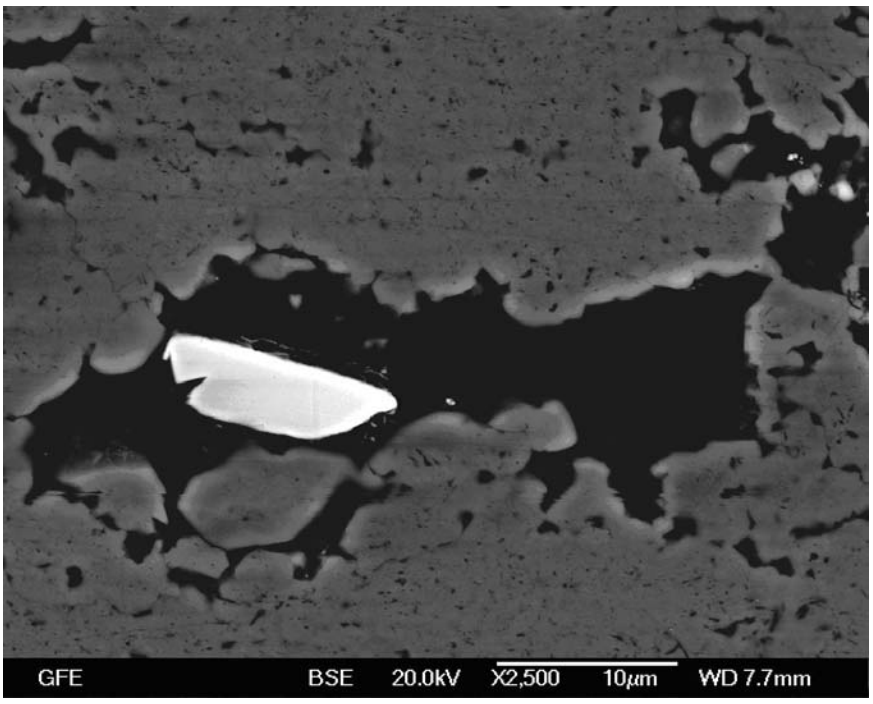

FIGURE 2. SEM backscatter image of tetrataenite crystal (lighter tone: whitish) within the cavity partially filled with Fe-chlorite (black). The surrounding mineral is magnetite (grey).

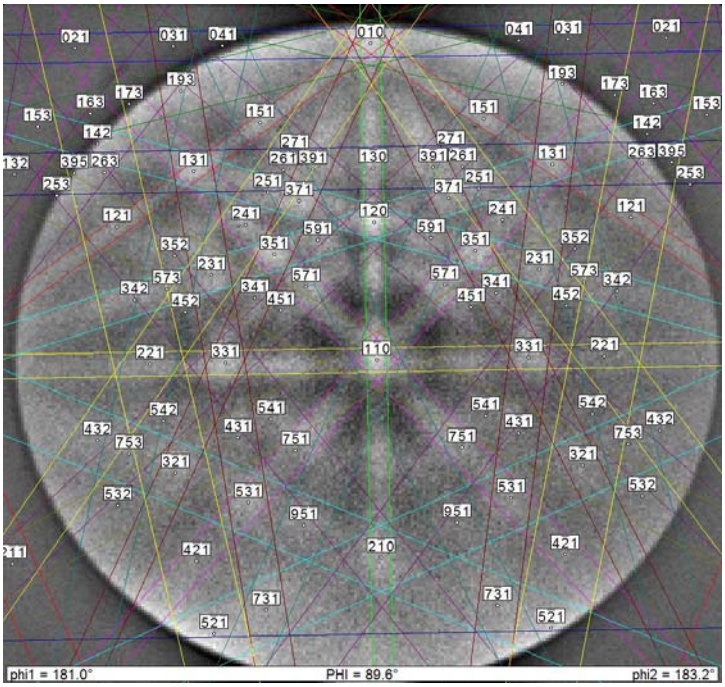

FIGURE 3. Electron backscatter diffraction (EBSD) Kikuchi pattern of tetrataenite crystal indexed with reference to American Mineralogist Crystal Structure (AMCS) Database.

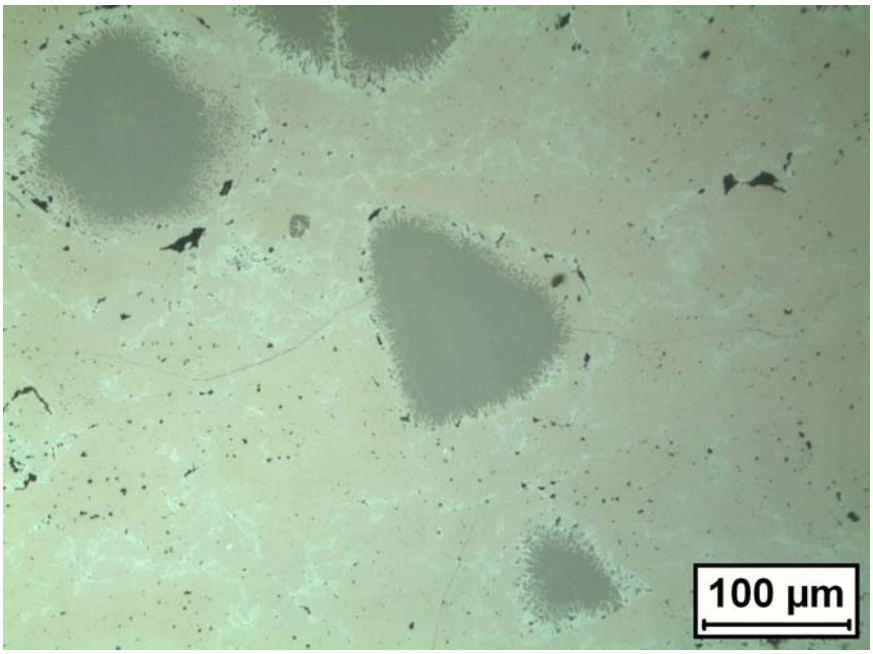

FIGURE 4. Magnetite (the main mass) replacing chromite grains (darker grey with corroded margins). Reflected plane polarized light.

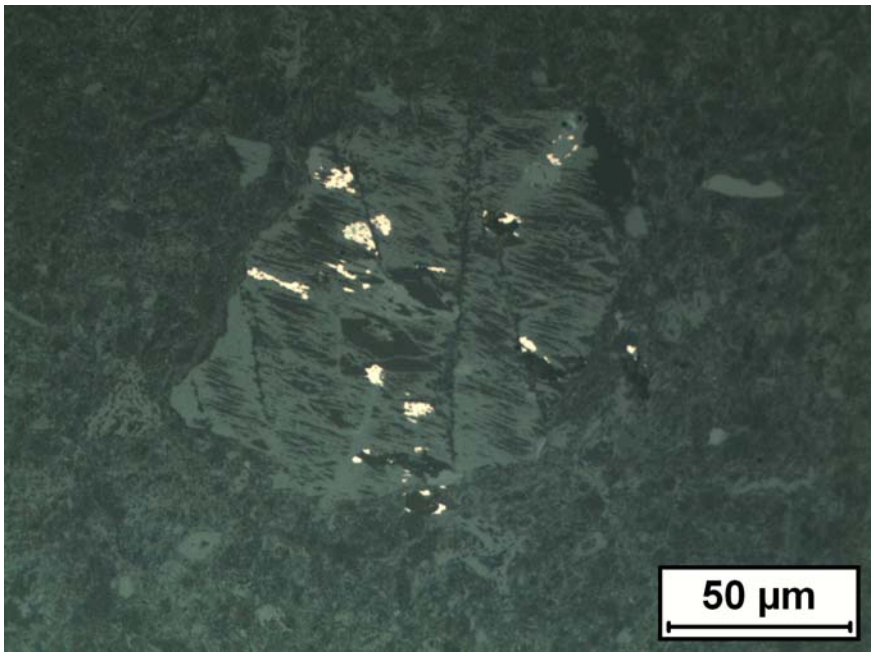

FIGURE 5. Occurrence of Cu-Fe alloy and non-stoichiometric Fe-Ni-Co -sulfide (high-reflectance) within highly altered Cr-Al spinel (centrally located bigger grain). The matrix is mostly Fe-chlorite with some relicts of altered spinel. Reflected plane polarized light.